Contents lists available at ScienceDirect

Heliyon

Binding domain on CD22 molecules contributing to the biological activity of T cell-engaging bispecific antibodies

Jie Chen [a], Zhidi Pan [a], Lei Han [d], Junjun Liu [a], Yali Yue [a], Xiaodong Xiao [c], Baohong Zhang [a], Mingyuan Wu [a], Yunsheng Yuan [a], Yanlin Bian [a], Hua Jiang [b,c], Yueqing Xie [c], Jianwei Zhu [a,*]

[a] Engineering Research Center of Cell and Therapeutic Antibody, Ministry of Education, School of Pharmacy, Shanghai Jiao Tong University, Shanghai, 200240, China
[b] Jecho Biopharmaceuticals Co., Ltd, Tianjin, 300450, China
[c] Jecho Laboratories, Inc., Frederick, MD21704, USA
[d] Jecho Institute, Shanghai 200240, China

A B S T R A C T

CD22, as the B-cell malignancies antigen, has been targeted for immunotherapies through CAR-T cells, antibody-drug conjugates (ADCs) and immunotoxins via interaction of antibodies with binding domains on the receptor. We hypothesized that avidity and binding domain of antibody to target cells may have significant impact on the biological function in tumor immunotherapy, and T cell-engaging bispecific antibody (TCB) targeting CD22 could be used in the therapy of hematologic malignancies. So, to address the question, we utilized the information of six previously reported CD22 mAbs to generate CD22-TCBs with different avidity to different domains on CD22 protein. We found that the avidity of CD22-TCBs to protein was not consistent with the avidity to target cells, indicating that TCBs had different binding mode to the protein and cells. *In vitro* results indicated that CD22-TCBs mediated cytotoxicity depended on the avidity of antibodies to target cells rather than to protein. Moreover, distal binding domain of the antigen contributed to the avidity and biological activity of IgG-[L]-scfv-like CD22-TCBs. The T cells' proliferation, activation, cytotoxicity as well as cytokine release were compared, and G5/44 BsAb was selected for further *in vivo* assessment in anti-tumor activity. *In vivo* results demonstrated that CD22-TCB (G5/44 BsAb) significantly inhibited the tumors growth in mice. All these data suggested that CD22-TCBs could be developed as a promising candidate for B-cell malignancies therapy through optimizing the design with avidity and binding domain to CD22 target in consideration.

1. Introduction

In recent years, immunotherapies have achieved breakthrough in the treatment of hematologic malignancies based on B-cell antigens [1–3]. However, only a few of patients had a response to these immunotherapies and the majority who did respond eventually would relapse due to the loss of the antigen, for example CD19 [4,5]. So exploring the vicarious targets may be a good choice, such as

BCMA, CD20, CD22. Among them, BCAM or CD20 have been targeted for the cancer therapy by constructing TCBs [6,7], and the corresponding products have been approved on market (Teclistamab, Mosunetuzumab and Glofitamab-gxbm). We want to explore the feasibility of the new target CD22 in TCB construction.

CD22 is a type 1 transmembrane sialoglycoprotein of the immunoglobulin (Ig) superfamily and consists of 7 extracellular Ig-like domains [8]. The N terminal of its extracellular domains could bind to sialic acid, and the other six C2-type Ig domains had no biological activity. CD22 was highly expressed on B cell-derived leukemic cells and restrictedly on normal B cells [9–11]. Due to its specific expression, CD22 has been targeted as one of the candidates for replacing CD19. To date, antibody therapies targeting CD22 on market have been the form of ADC (Inotuzumab Ozogamicin) and immunotoxin (Moxetumomab pasudotox). Anti-CD22 CAR-T cells therapy has also been validated as a promising agent for B-cell leukemia in several clinical trials [12,13]. Moreover, with the ability to recruit and activate T cells, TCBs targeting CD22 is worthwhile explored as being on clinical trial (NCT04540796). Due to no complete available clinical trial report, it was worthy to make a further study to illustrate the mechanism of anti-tumor activity of CD22-TCBs.

TCB elicited immune activity by simultaneously binding to CD3 on T lymphocytes and antigen on target cells, which induced the activation, cytotoxicity and proliferation of T cells [14–16]. More and more evidences appeared that appropriate intercellular distance between T cells and target cells mediated by TCBs had significant impact on T cells activity [17,18]. Usually, a close proximity of target and effector cells was conducive to the formation of a tight immune synapse and induces strong immune activity [19–22]. Other studies also revealed that CAR-T and TCR-T immunotherapies targeting the proximal domain of CD22 protein demonstrated superior biological activity compared with other binding domains [12,23]. However, for TCBs targeting CD22, the question would be if TCB targeting proximal domain mediated better activity than TCB targeting distal domain? To address this question, we designed and constructed six CD22-TCBs with different avidity and binding domains to evaluated their biological activity.

Previous study confirmed that TCB with IgG-[L]-scfv structure had the best anti-tumor activity than BiTE and IgG structure [18], which was also proved by TCBs targeting CD33, Her2 and GPA33 [24–26]. So, we also used this format to construct CD22-TCB. The sequences of Fabs targeting CD22 were derived from different anti-CD22 antibodies sequences in human IgG1, κ, and the anti-CD3 scfv was fused to the C terminal of each light chain. The sequences of six anti-CD22 antibodies came from the IgGs or scfvs of G5/44 [27], HLL2 [28,29], BL22 and HA22 [30,31], M971 and M972 [32].

In this study, we have constructed six CD22-TCBs (named G5/44 BsAb, HLL2 BsAb, BL22 BsAb, HA22 BsAb, M971 BsAb, M972 BsAb), and performed binding and cytotoxicity measurements, activation, cytokines release, proliferation and internalization assays. Among six CD22-TCBs, G5/44 BsAb with distal binding domain had high avidity to target cells, and had the best *in vitro* biological activity. It also inhibited tumor growth in Raji xenograft model. This work provided a direction for optimizing TCB targeting CD22 and CD3, and proved the feasibility of this agent in cancer therapy.

2. Materials and methods

2.1. Cell lines

Raji and K562 cells were stored in the cell bank of our laboratory and were originally from a gift of Dr Wei Han MD, PhD in School of Pharmacy of Shanghai Jiao Tong University. Reh cells were purchased from Chinese Type Culture Collection. NALM-6G cells were a gift from Dr Dengli Hong MD, PhD in School of Medicine of Shanghai Jiao Tong University. All cell lines were cultured in RPMI 1640 medium with 10% fetal bovine serum and 1% penicillin-streptomycin at 37 °C in 5% CO_2.

2.2. Vectors construction and CD22-TCBs production

The sequences of variable heavy (V_H) and light (V_L) chains derived from six anti-CD22 antibodies (G5/44 and HLL2 from US20160015831A1, BL22 and HA22 from US9868774B2, M971 and M972 from US9598492B2) were constructed into the human IgG1 with LALA-PG mutations [33]. Then anti-CD3 scfv, derived from huOKT3 [34], was fused by a linker of three G_4S_1 domains. The V_H and V_L domains of the scfv were linked by an additional six G_4S_1 domains. The final sequences were constructed and transfected into HEK 293F cells [35–38], which was different to our experience in clinical-grade production of HA22 [39]. Next, the proteins were purified by affinity chromatography (MabSelect SuRe). Purified CD22-TCBs were detected by SDS-PAGE and dialyzed into phosphate buffer saline (PBS).

2.3. Avidity assay of CD22-TCBs to CD22 protein

Biosensor analysis was performed using Biacore 8K (GE Healthcare Bio-Sciences AB, Uppsala, Sweden) on streptavidin chip (SA chip, GE). The chip was first flowed with 1 M NaCl/50 mM NaOH under the flow rate of 10 μL/min with 60 s for three times. Then the biotinylated Fc conjugated human siglec-2/CD22 protein (Cat. No. SI2-H82F8, ACROBiosystems) was coupled to the surface of SA chip by the link to SA with 5 μg/mL for 120 s. Finally, the chip was washed by 50% isopropanol in 1 M NaCl/50 mM NaOH solution. After the conjugation of CD22 protein to SA chip, CD22-TCBs were double diluted in HBS buffer (10 mM HEPES, pH 7.4, 150 mM NaCl, 3.4 mM di-Na-EDTA, and 0.005% Tween 20), and aliquots (118 μL) were injected over the sensor chip surface at a flow rate of 30 μL/min for 120 s. After the injection phase, dissociation was monitored by flowing HBS buffer over the chip surface for 120 s. Bound CD22-TCBs were eluted, and the chip surface was regenerated by the injection of glycine pH 1.5 with 30 μL/min for 30 s. Apparent ka and kd constants were calculated by nonlinear least squares regression analysis, using Biacore Insight Evaluation 2.0.15.12933.

2.4. Bioactivity of the CD22-TCBs

Cell binding assay was performed to evaluate the bioactivity of six CD22-TCBs by using CD22$^+$ NALM-6G cell line. In brief, NALM-6G cells were harvested in logarithmic phase with 5E5/well, and incubated with 5 μg CD22-TCB on ice for 30 min. After incubation, samples were incubated with secondary antibody (APC conjugated anti-human IgG Fc Antibody, Biolegend™) under the same condition. Finally, samples were analyzed by CytoFLEX cytometry.

2.5. Avidity assay of CD22-TCBs to target cells

CD3$^+$ Jurkat cells and three CD22$^+$ cell lines (Raji, Reh and NALM-6G) were selected to detect binding ability of six CD22-TCBs. The methods were the same as before (2.4 in "Materials and methods"). Cells were harvested and equalized into round 96-well. For Jurkat cells, CD22-TCB was 5-fold diluted from 500 nM to 0.032 nM. For CD22$^+$ cells, CD22-TCB was 5-fold diluted from 100 nM–0.0064 nM. After incubation, samples, except NALM-6G cells, were incubated with FITC conjugated goat anti-human IgG (H + L) secondary antibody (ThermoFisher™). NALM-6G samples were incubated with PE conjugated goat anti-human IgG Fc secondary antibody, (eBioscience™). Finally, all samples were analyzed by CytoFLEX cytometry. Median fluorescence intensity (MFI) was counted and analyzed by GraphPad Prism.

2.6. In vitro cytotoxicity mediated by huPBMCs

Target cells (Raji, Reh, NALM-6G and K562) were seeded on culture plates with 1000 rpm, 1 min. All measurements were done in duplicate, and the method was according to previous published article [40].

2.7. CD69, CD25 expression and cytokine detection

The supernatant from the cytotoxicity was collected and detected using human IL-2 and IFN-γ ELISA kit (R&D Systems, Inc.). Cells were analyzed by flow cytometry either using CD8-FITC, CD4-PE (Sino Biological) and CD69-APC mAbs (BD Biosciences) or using CD8-FITC, CD4-PE and CD25-APC mAbs (Sino Biological) to detect the expression of CD69 and CD25. Finally, CD69$^+$ and CD25$^+$ percentages, as well as MFI on CD8$^+$ and CD4$^+$ T cells was counted and analyzed by GraphPad Prism.

2.8. T cell proliferation assay

CFSE-labeled huPBMCs were incubated with Raji cells with a ratio of 10:1, and treated with 1000 ng/mL CD22-TCB at 37 °C. Next, the cell mixture was harvested on day 2, 4 and 6 with labeling of mouse anti-human CD3 APC-labeled mAb (Sino Biological). Percentage of proliferation was calculated and analyzed by the low fluorescence intensity.

2.9. Cell-cell association assay

CFSE labeled Raji cells and PKH26 (Sigma; PKH26GL) labeled Jurkat cells were mixed at equal ratio (2×10^6/mL) in the presence of CD22-TCB (100 ng/mL) or not. The experiment method and analysis method were referring to previous report [41].

2.10. Autologous B-cell depletion mediated by CD22-TCBs in vitro

Fresh isolated huPBMCs (2E6 cell/mL, 100 μL) were incubated with 1 μg/mL CD22-TCB or not at 37 °C. Next, the cells were collected on 20, 46 and 70 h with labelling of PE conjugated anti-human CD20 mAb (Sino Biological) at 4 °C for 30 min, and then analyzed as previously reported [42]. Percentage of CD20$^+$ B cells was quantified and analyzed by GraphPad Prism.

2.11. Internalization to Raji cells

For the time course of internalization, Raji cells were incubated with 5 μg/mL FITC-labeled CD22-TCB at 37 °C and 4 °C respectively for 0.25, 0.5, 1, 2, 3 and 4 h. The cells were then stripped with 0.2 M glycine buffer pH2.5 containing 1 mg/mL BSA to remove surface-bound CD22-TCB. The saturated surface-bound amount was conducted with G5/44 BsAb at 4 °C for 30 min due to the highest binding to Raji cells. Internalization percentage was measured by flow cytometry and calculated as following: Internalization% = (median fluorescence intensity (MFI) at 37 °C - MFI at 4 °C)/(MFI of G5/44 BsAb at 4 °C for 30 min).

2.12. In vivo anti-tumor activity

SPF-grade NOD/SCID female mice, aged 6–8 weeks, were obtained from Beijing Vital River Laboratory Animal Technology Co., Ltd., and kept in SPF-grade animal room of Laboratory Animal Center of Shanghai Jiao Tong University. The temperature, relative humidity and light/dark cycle respectively were 24 ± 2 °C, 60% ± 2%, and 12/12 h. The bedding, food and drinking water were all sterilized. Raji cells (5E6 cells) were admixed with huPBMCs (5E6 cells). Then, the cells mixture was injected s.c. in mice with 0.1 mL RPMI medium. Therapy administration (PBS or 5 mg/kg G5/44 BsAb) was performed on day 0, 4 and 7–12 days by tail vein injection.

Tumor size was measured and calculated as following: $V = 0.5 \times (\text{length} \times \text{width} \times \text{width})$. After the tumor size reached 1000 mm³, mice were euthanized.

2.13. Animal experiment statement

The authors declared that the experimental protocol in animal study was approved by Institutional Animal Care and Use Committee of Shanghai Jiao Tong University, as the approval number was A2018041. All methods were conducted in accordance with the guidelines from the Institutional Animal Care and Use Committee of Shanghai Jiao Tong University. Informed consent was obtained from all participants donating blood.

3. Results

3.1. Generation of six CD22-TCBs

All six CD22-TCBs were constructed and purified as described in "Materials and methods". All six CD22-TCBs appeared corresponding bands under the non-reducing and reducing condition (Fig. S1). The fusion of huOKT3 scfv contributed to an increased molecular weight of light chain. From this result, all CD22-TCBs were well generated and would be evaluated in the following *in vitro* and *in vivo* assays.

3.2. Comparison of biochemical activities of six CD22-TCBs

We first performed the binding activity of purified CD22-TCBs to NALM-6G cells due to the expression of CD22 on cell surface [12]. Flow cytometry assay demonstrated that all CD22-TCBs could bind to NALM-6G cells (Fig. 1A) even though they bound to different domains on CD22 protein (Fig. 1B). Among them, G5/44 BsAb binds to domain 1 that located on the furthest position to the membrane. HLL2 BsAb binds to domain 2. BL22 and HA22 BsAbs bind to the same domain 3 that is nearer to membrane than G5/44 and HLL2 BsAbs. M971 and M972 BsAbs bind to domain 7 that is nearest to membrane.

The kinetic analyses were performed to detect binding dynamics of six CD22-TCBs to CD22 protein. Results showed that HA22 BsAb had the highest avidity with 1.16E−12 M due to the smallest kd (9.12E−07 M). Avidity measurement results were listed in Table 1 and Fig. S2. G5/44 BsAb had a high kd and modest ka, which resulted in low avidity. M971 BsAb also had a high kd and ka, leading to its KD of 1.60E−09 M. In this assay, HA22 BsAbs had a higher avidity than BL22, which was consistent with previous research [43]. M971 and M972 BsAbs showed no significant difference in avidity to CD22 protein compared to IgG1-like M971 and M972 [32]. However the avidity of G5/44 and HLL2 BsAbs was lower than the reported value (g5/44, 0.07 nM [27] and HLL2, 0.7 nM [44]), which might be due to low amount of CD22 protein immobilized on chip in our assay.
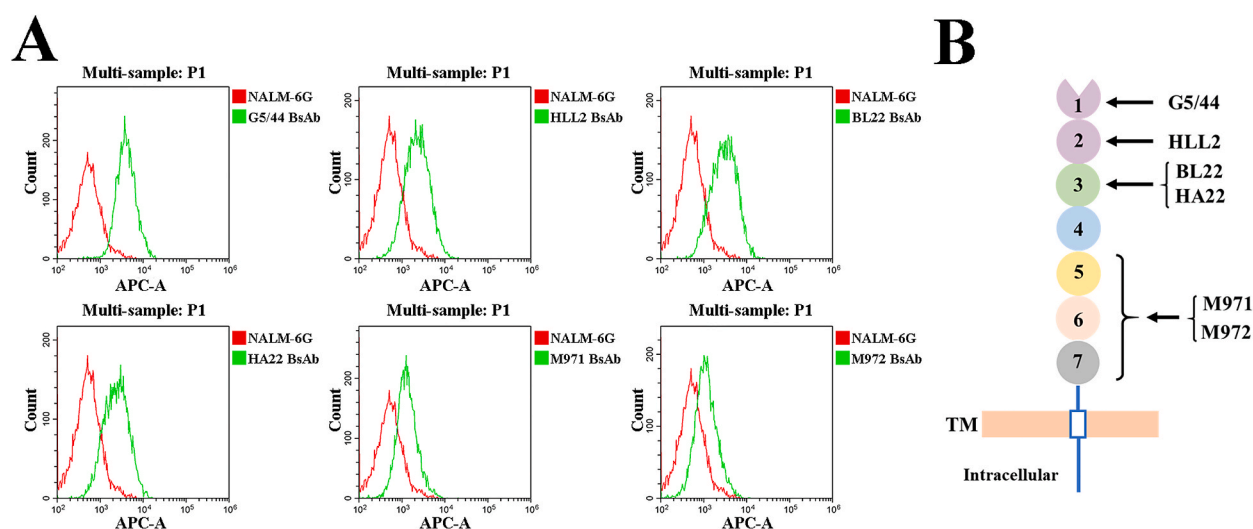

Fig. 1. Binding to NALM-6G cells and different binding domains on CD22 molecule. (A) FACS histograms of six CD22-TCBs binding to NALM-6G cells. Red line is the fluorescence signal of target cell NALM-6G and green line is the fluorescence signal of CD22-TCB. (B) Different binding domains of six CD22-TCBs on CD22 molecule. G5/44 BsAb binds to domain 1, HLL2 BsAb binds to domain 2, BL22 and HA22 BsAbs bind to domain 3, M971 and M972 BsAbs bind to domain 7. (For interpretation of the references to colour in this figure legend, the reader is referred to the Web version of this article.)

Table 1
Binding parameters of six BsAbs to CD22 molecule.

BsAbs	ka (1/Ms)	kd (1/s)	KD (M)
G5/44	1.74E+05	9.85E−03	5.66E−08
HLL2	2.55E+04	6.35E−05	2.49E−09
BL22	1.70E+06	9.39E−04	5.53E−10
HA22	7.88E+05	9.12E−07	1.16E−12
M971	1.95E+06	3.13E−03	1.60E−09
M972	1.67E+06	5.11E−04	3.06E−10

3.3. Binding ability of CD22-TCBs to CD22$^+$ B cells

To assess biological activity of six CD22-TCBs, binding ability to CD22$^+$ B cells was firstly analyzed by flow cytometry assay (Fig. 2A). In this result, G5/44, BL22 and HA22 BsAbs had the best binding activity to Raji, Reh and NALM-6G cells with sub-nanomolar level (EC_{50} = 0.3–0.8 nM), followed by HLL2 BsAb (EC_{50} = 6.92–19.28 nM) (Table S1). However, M971 and M972 BsAbs had the lowest binding activity (EC_{50} = 17.7–202.7 nM), and had low binding ability even at high concentrations of 100 nM. Flow cytometry assessment of the binding activity against CD22 positive cells for BL22 and HA22 BsAbs was consistent with the biacore data. But we found that G5/44 BsAb had a lower EC_{50} value at sub-nanomolar level, with a higher avidity constant (KD = 5.66E−08 M) due to its high kd (kd = 9.85E−03 1/s) (Table 1). This might be owing to the nanoclusters formation of CD22 on B cell surface, which was benefit for the binding of G5/44 BsAb to epitope A on the first N-terminal domain [27,45]. The low avidity of M971 and M972 BsAbs to target cells might also be due to the nanoclusters formation which hindered the membrane proximal binding domain of M971 and M972 BsAbs [12]. These results showed that the avidity of an antibody to protein was not always consistent with the avidity to target protein on cells. So binding kinetics to protein or to cells should both be considered during antibody design, as a target protein can be in circulation system or uneven on a cell surface. In another hand, six CD22-TCBs had similar binding activity to CD3$^+$ Jurkat cells, as the same anti-CD3 scfv was used to construct TCBs.

3.4. In vitro cytotoxicity

To evaluate cytotoxicity activity of six CD22-TCBs, freshly isolated huPBMCs were used as effector cells to mediate redirecting immune cell killing against CD22$^+$ malignant B-cell lines. For CD22$^+$ B-cell lines, the CD22-TCBs (G5/44, HLL2, BL22 and HA22 BsAbs) with high avidity to cells had the better cytotoxicity than the CD22-TCBs (M971 and M972 BsAbs) with low activity to cells (Fig. 2B). For CD22 negative B-cell line, all CD22-TCBs had some cytotoxicity at high concentration, which was possible due to the non-specific cytotoxicity mediated by T cells or the cytotoxicity to normal B cells in huPBMCs. For high CD22-expressing Raji cells, G5/44 and BL22 BsAbs achieved the lowest EC_{50} among all CD22-TCBs (separately 9.977 and 8.376 ng/mL), followed by HA22 BsAb (23.29 ng/mL) and HLL2 BsAb (37.79 ng/mL) (Table S2). M971 BsAb achieved a low EC_{50} (65.71 ng/mL), and had a low cytotoxicity window. M972 BsAb had a much higher EC_{50} (467.1 ng/mL) with a very low cytotoxicity window. From these data, TCBs with high binding ability to CD22 positive cells had a high killing cytotoxicity, even though the binding domain of this TCB was far away from cell membrane. For CD22-TCBs with the same binding domain, BL22 BsAb had a lower EC_{50} cytotoxicity than HA22 BsAb due to its lower
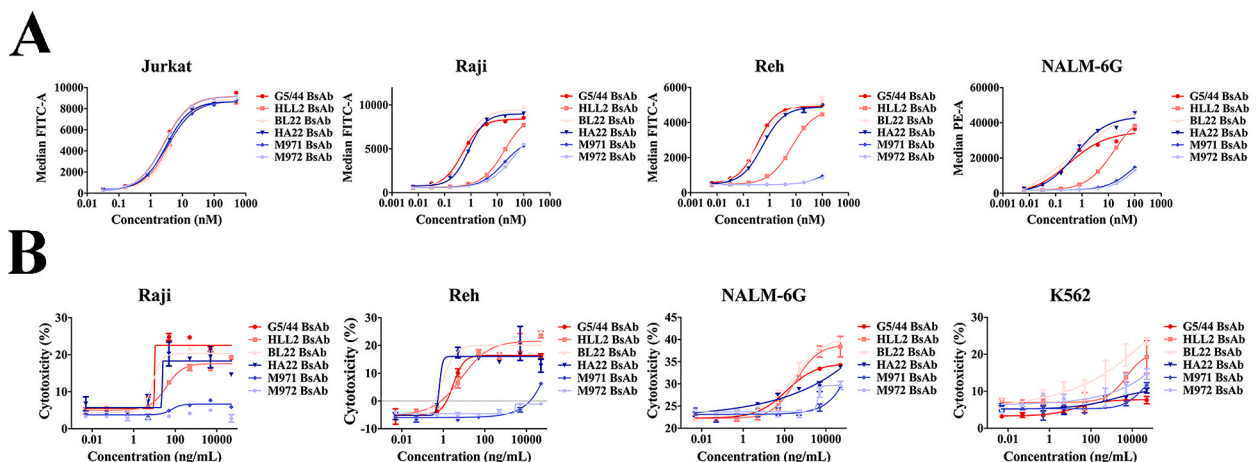

Fig. 2. Binding affinity and cytotoxicity to cells of six CD22-TCBs. (A) Binding affinity to Jurkat, Raji, Reh and NALM-6G cell lines. Cell binding activity of six CD22-TCBs against target cells was measured by flow cytometry. Geometric MFI was calculated at different concentration and analyzed by GraphPad Prism. (B) Cytotoxicity to target cells. Detection of LDH release after freshly isolated huPBMCs incubated with target cells at 10:1 ratio (Effector:Target) for about 60 h under the different concentration of CD22-TCBs. Data were shown as means ± SD (n = 2).

binding EC_{50} to Raji cells. All these results proved that high binding ability of CD22-TCB to target cells could contribute to its biological activity.

3.5. CD69 and CD25 expression on T cells

As previously reported, TCB could activate T cells to express CD69 and CD25, which played an important role in T cells mediated cytotoxicity [46]. After 23 h incubation, the ratios of $CD69^+$ T cells in $CD8^+$ and $CD4^+$ T cells were obviously increased in G5/44, HLL2, BL22 and HA22 BsAbs groups. In contrast, the ratios were increased significantly less in M971 and M972 BsAbs groups (Fig. 3A). Further, the expression levels of CD69 on $CD8^+$ and $CD4^+$ T cells in G5/44, HLL2, BL22 and HA22 BsAbs groups were much higher than that in M971 and M972 BsAbs groups. Interestingly, $CD8^+$ and $CD4^+$ T cells almost had no CD69 expression under the low concentration of all CD22-TCBs, but with high CD69 positive percentage. This might be because of the auto-activation of T cells by target cells (Raji). By the analysis of CD25 expression on T cells, both M971 and M972 BsAbs had a very weak T cells activation with a low CD25 expression (Fig. 3B). Nevertheless, G5/44, HLL2, BL22 and HA22 BsAbs had the ability to consistently activate T cells with no obvious difference on CD25 positive percentage on $CD8^+$ and $CD4^+$ T cells, but with notable difference on CD25 expression intensity. This suggested that these four BsAbs had similar ability to activate T cells but different to induce CD25 expression. This assay showed that T cells activation level induced by CD22-TCBs was consistent with cytotoxicity, and also demonstrated that TCBs targeting CD22 antigen not only could induce the T cells activation, but also had various activation ability based on different avidity to target cells.

3.6. Cytokines release and T cell proliferation

Cytokines play an important role in cancer treatment by regulating immune response [47]. Cytokine release is the mechanism of action of TCBs in anti-tumor activity, as proved by other studies [6,40]. To further evaluate activation ability of six CD22-TCBs, IL-2 and IFN-γ detection assays were performed. We found that G5/44 BsAb could induce the highest IL-2 secretion, followed by BL22, HA22 and HLL2 BsAbs, but not seen with M971 and M972 BsAbs (Fig. 4). Likewise, only G5/44, BL22, HA22 and HLL2 BsAbs could induce dose-dependent IFN-γ release, but with different release amount. Interestingly, G5/44 BsAb had the stronger ability to promote the release of IL-2 and IFN-γ than BL22 BsAb, even though they had similar binding affinity and cytotoxicity to target cells.

T cells activation induced by TCBs contributed to T cells proliferation, and promoted the anti-tumor activity [16,48]. So the proliferation of T cells is also an index to evaluate the activation ability of CD22-TCBs. After two days' activation, T cells in G5/44, HLL2, BL22 and HA22 BsAbs groups had a nearly 20% proliferation percentage (Fig. 5A and B). However, four days later, the proliferation difference was widened among six CD22-TCBs. Six days later, the proliferation ratios did not increase in G5/44, BL22, HA22 and HLL2 BsAbs groups, except for M971 and M972 BsAbs groups with a small increase. By cytokines release and proliferation assays, it could be concluded that G5/44 BsAb in all six CD22-TCBs appeared promising potential for treatment of B-cell associated diseases.

In previous results, we found that the percentage of $CD69^+CD8^+$ cells in $CD8^+$ T cells and $CD69^+CD4^+$ cells in $CD4^+$ T cells achieved 70% and 60% when under the very low concentration of six CD22-TCBs (Fig. 3A). To further explore the possible mechanism of the observation, we analyzed the effect of CD22-TCBs or target cells on T cells activation (Fig. 5C). G5/44, HLL2, BL22 and HA22 BsAbs alone could activate T cells and upregulated CD69 expression on $CD8^+$ and $CD4^+$ T cells, but not M971 and M972 BsAbs. Target cells (Raji) alone could also activate CD69 expression as well on $CD8^+$ and $CD4^+$ T cells with more than 20% proliferation percentage. This result indicated that T cells could be activated at low concentration of BsAbs in the presence of target cells (Raji). But only in the
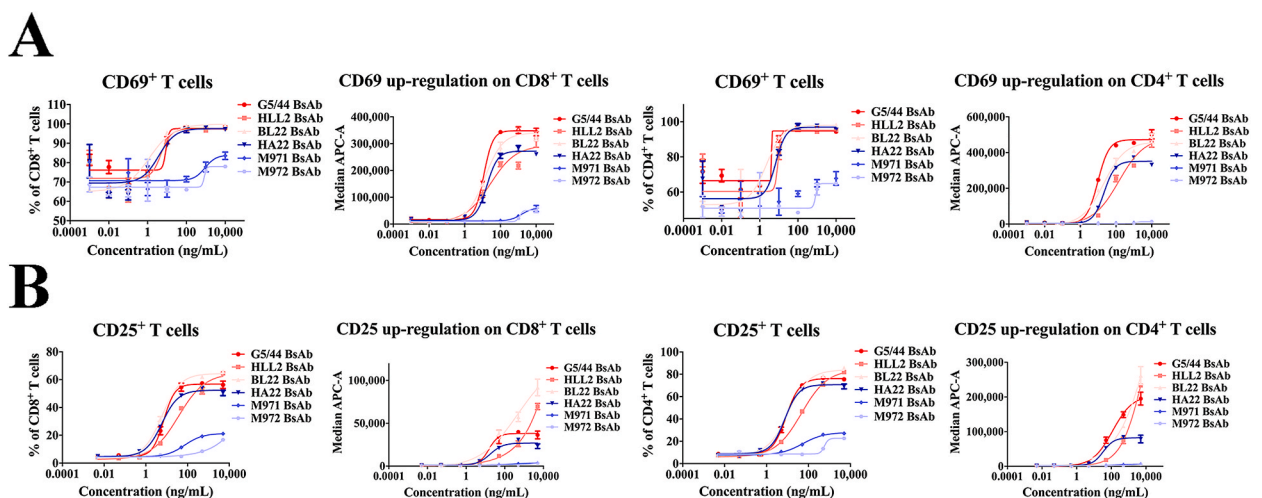

Fig. 3. Activation assay of CD69 and CD25 expression on T cells. (A) CD69 expression frequency and intensity on $CD8^+$ and $CD4^+$ T cells analyzed after 23 h incubation. (B) CD25 expression frequency and intensity on $CD8^+$ and $CD4^+$ T cells analyzed after 66 h incubation. Data were shown as mean ± SD (n = 2).
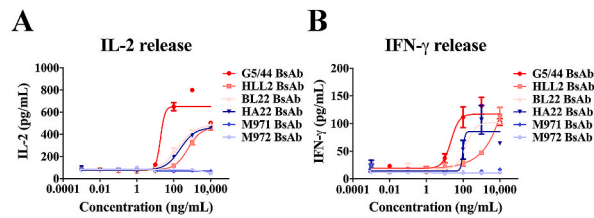
Fig. 4. Cytokine release of IL-2 and IFN-γ mediated by six CD22-TCBs *in vitro*. Detection of IL-2 (A) and IFN-γ (B) was performed by ELISA with different drug concentration and analyzed by GraphPad Priam. Data were shown as mean ± SD (n = 2).
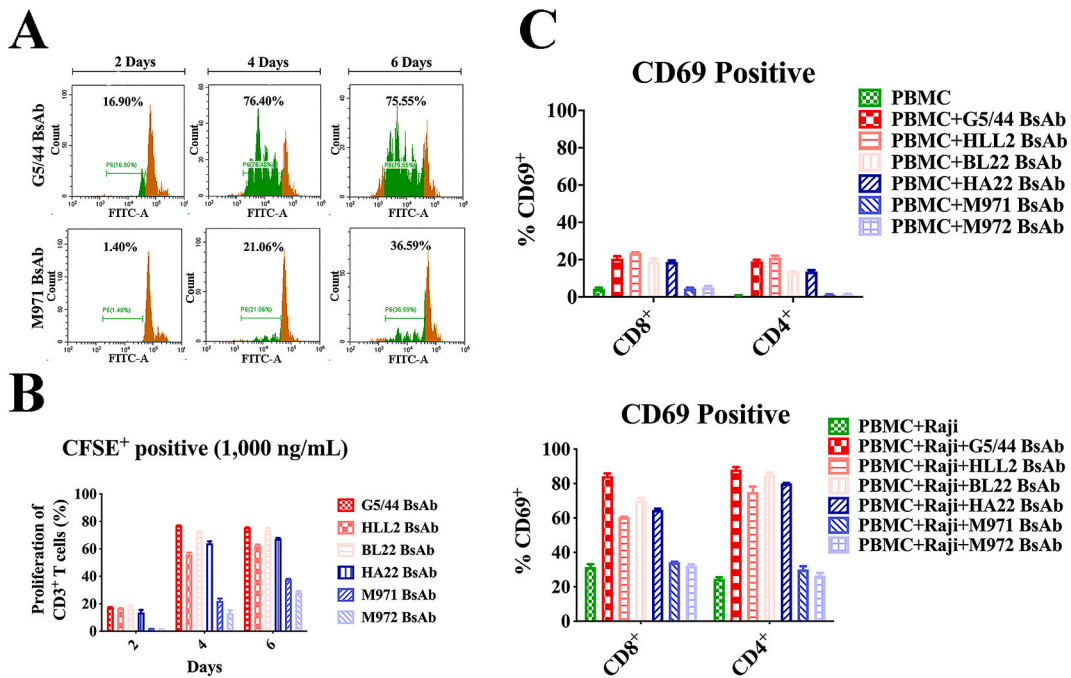

Fig. 5. CD3$^+$ T cells proliferation and CD69 expression frequency on CD8$^+$ and CD4$^+$ T cells. (A) FACS histograms of CD3$^+$ T cells proliferation for G5/44 BsAb (up line) and M971 BsAb (next line) on 2, 4 and 6 days. Green signal was the proliferated CD3$^+$ T cells with the lower fluorescence intensity contributed by CD22-TCBs. (B) Column diagram of CD3$^+$ T cells proliferation mediated by all six CD22-TCBs. (C) Expression frequency of CD69 on CD8$^+$ and CD4$^+$ T cells after 20 h incubation of huPBMCs with presence or absence of Raji cells or 100 ng/mL CD22-TCBs. Data were shown as mean ± SD (n = 3). (For interpretation of the references to colour in this figure legend, the reader is referred to the Web version of this article.)
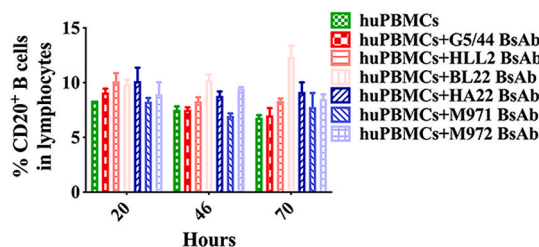

Fig. 6. Autologous B-cell depletion. Percentage of CD20$^+$ B cells in huPBMCs treated by CD22-TCBs. Data were shown as mean ± SD (n = 3).

presence of both CD22-TCBs and target cells, CD8$^+$ and CD4$^+$ T cells could be maximally activated with nearly 60–80% percentage of CD69$^+$ T cells (Fig. 5C).

3.7. Autologous B-cell depletion mediated by CD22-TCBs

Due to CD22 expression on B cells in huPBMCs [9], we performed autologous B-cell depletion assay mediated by six CD22-TCBs to evaluate their potential toxicity. With a final concentration of 1 μg/mL, all six CD22-TCBs almost had no impact on CD20$^+$ B cells quantity from 20 h to 70 h (Fig. 6). The data suggested that six CD22-TCBs almost had no toxicity to normal B cells in huPBMCs, and CD22 protein was a suitable target for the therapy of B-cell diseases due to its high expression (60–90%) on B-cell malignancies [49].

3.8. Cell-cell association and internalization mediated by CD22-TCBs

TCB could mediate the association of T cells and target cells to activate T cells, and activated T cells sequentially released perforin, granzyme and cytokines to kill tumor cells [50]. We used Jurkat cells evaluate recruiting ability of six CD22-TCBs, and found that BL22 BsAb exhibited a clear cell-cell association, followed by HA22, G5/44, HLL2, M972 and M971 BsAbs (Fig. 7A). Due to the 2.84% population in "No BsAb" group, it meant that Raji cells and Jurkat cells had a spontaneous cell-cell association. The cell association of T cells and target cells mediated by CD22-TCBs proved its binding ability to cells, which contributed to specific target cells lysis as previously reported [51].

Many studies had proved that antibodies targeting CD22 could be internalized into cells [30,52,53], which was beneficial to immunotoxin-based drug design and antibody-drug conjugate. Internalization assay revealed that G5/44, BL22, and HA22 BsAbs were internalized rapidly within 1 h incubation, and achieved the maximal internalization (about 80%) in 2 h (Fig. 7B). However, HLL2 BsAb only had a moderate internalization rate around 40% at maximum. M971 and M972 BsAbs had the lowest internalization rate around 20% at maximum. Internalization of CD22-TCBs evaluated by MFI also validated this result (Fig. 7C). This result suggested that CD22-TCBs with high avidity to cells possibly led to high internalization rate (G5/44, BL22, and HA22 BsAbs). This phenomenon was also confirmed by different internalization rate between BL22 and HA22 (scfv-like structure). HA22 had a higher internalization rate than BL22 [54].

3.9. In vivo anti-tumor activity mediated by G5/44 BsAb

There is no research report about the biological activity of CD22-TCB, as well as its anti-tumor activity. To confirm the potential feasibility of CD22-TCB used in immunotherapy, we further studied its anti-tumor activity in *in vivo* xenografted animal model. Comparing the *in vitro* activity of six CD22-TCBs, G5/44 BsAb was selected for the *in vivo* study to evaluate the anti-tumor activity. Although with no Fc function, G5/44 BsAb could significantly inhibit the tumor growth compared with PBS group (Fig. 8), which demonstrated the potential anti-tumor activity of TCB targeting CD22. Previous study reported that treatment with parent g5/44 mAb (the variable domains of G5/44 BsAb targeting CD22 with human IgG4 constant framework) with 8 mg/kg dosage had no effect on the tumor growth of Ramos BCL [27], which might be due to the lack of Fc function. The significant inhibition of tumor growth by G5/44 BsAb indicated that the anti-tumor activity of CD22-TCB was dependent on the binding of anti-CD3 scfv to T cells, and revealed that CD22-TCB could be further explored in the immunotherapy of B-cell associated diseases.

4. Discussion

CD22, a B-cell surface antigen, is highly expressed by B-cell malignancies, such as lymphoblastic leukemia and lymphoma [55].
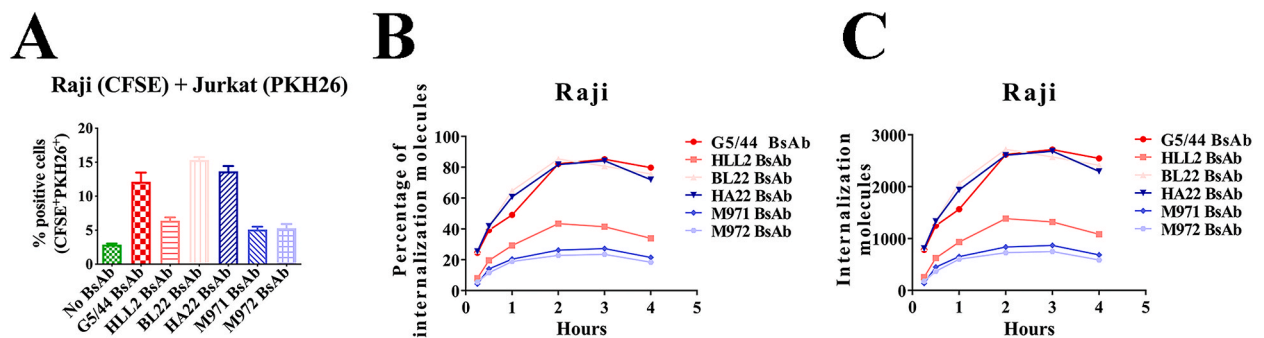

Fig. 7. Cell-cell association and internalization of Raji cells mediated by six CD22-TCBs. (A) The Jurkat-Raji cell-cell association mediated by six CD22-TCBs. The association population was determined using flow cytometry and quantified as the percentage of positive cells in the upper right quadrant of FITC-A versus PE-A, and data were analyzed by GraphPad Prism and shown as mean ± SD (n = 3). (B) Internalization percentage of six CD22-TCBs with time course. (C) Internalized molecule amount of six CD22-TCBs with time course. The experiment of internalization was repeated with one time.
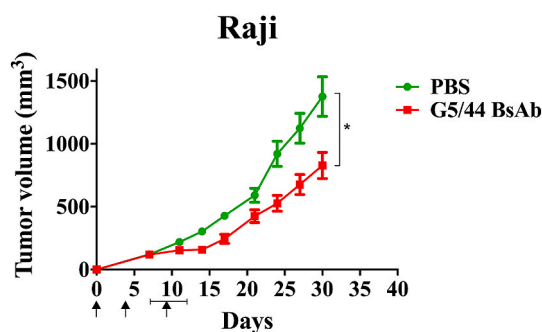
Fig. 8. Time course of tumor growth curve. Arrows were indicated that mice were treated with 5 mg/kg G5/44 BsAb or PBS on day 0, 4 and 7–12 days. Significant difference analysis of BsAb group to PBS group was analyzed by two-way ANOVA analysis using Sidak's multiple comparisons test with a single pooled variance. Data were shown as means ± SD (n = 5). **** means $p < 0.0001$.

Two drugs targeting this antigen were approved on the market (Inotuzumab Ozogamicin [52] and Moxetumomab pasudotox [56]). In addition, more than 100 immunotherapies targeting CD22 with different avidity and binding epitopes are currently in clinical trials (https://clinicaltrials.gov). It is worthwhile to review and evaluate the effect of avidity, binding domain and internalization attributes of TCBs on their biological activity comprehensively. In this report, we presented initial exploration on the assessment from multiple angles and meanwhile, we proposed a number of CD22-TCBs with potential demonstrated efficacy for treatment of hematological malignancies.

M971 BsAb, with a high avidity to CD22 antigen, had a low avidity to target cells, which revealed the differences of the avidity between the antibody to the target protein and the target protein on cells. This phenomenon was also confirmed by P-cadherin-TCB [57]. In that report, 20 DART and 30 DART had high avidity to P-cadherin protein, while with low avidity to target cells. PF DART and 20 DART which sharing the same binding domain of P-cadherin, had same avidity to the protein but significant different avidity to target cells. All these results including ours proved that the differences between antibody avidity to the target protein and target cells should be well characterized during TCB development.

In vitro activity of CD22-TCBs was dependent on the avidity to target cells, suggesting that the avidity of the antibody to the cell surface played a crucial role in the cell lysis of a TCB, as observed in previous report about P-cadherin-TCB [57]. When P-cadherin-TCB with distal binding domain had a higher avidity to target cells, it also had a higher cytotoxicity than P-cadherin-TCB with proximal binding domain.

In our study, we found that binding of the TCB to a distal binding domain had significant impact on its biological activity. However, it may depend upon the structure of an antibody. Proximal binding domain of MCSP-TCB and EpCAM-TCB in one study using BiTE-like structure [22] had good target cells lysis. This might be due to its small molecular weight and the high affinity to target cells. Another study revealed that FcRH5-TCB (1G7) binding to the proximal domain of FcRH5 more efficiently led to synapse formation than TCBs with the central or distal domains [20].

The cluster of CD22 on the target cells was mediated by the ligand of CD22, rather than CD22-TCB. The proximal binding domain of the cell surface antigen could be hided inside of the cluster, which prevented the TCBs with large molecular weight binding to the domains. Due to the present of cluster, IgG-[L]-scFv-like CD22-TCB with large molecular weight might bind easy to the distal binding domain. So G5/44, HLL2, BL22 and HA22 BsAbs had better binding activity than M971 and M972 BsAbs in our study. In the other case, TCBs with small molecular weight (DART, BiTE) or nanobody structure [58,59] might bind to the covert epitope on the antigen, and maintained the avidity to the target cells. So in the further study, we would need to design and construct CD22-TCBs adopting these structures to evaluate the binding activity to target cells.

Previous report proved that CD22 targeted CAR-T therapy with a proximal binding domain had better therapeutic effectivity to treat B-cell acute lymphoblastic leukemia than that with a distal binding domain [12]. This revealed that binding domain played a dominant role in CAR-T therapy rather than the avidity. Whereas, our data demonstrated that distal binding domain of IgG-[L]-scfv-like CD22-TCB contributed to the high avidity to target cells. It reveals that there are differences between CAR-T therapy and TCB therapy. The differences might due to different mechanism of the actions. In CAR-T therapy, when the antibody on the CAR-T bind to the target cells, the T cells will be activated immediately, despite with a low avidity. However, in the TCB therapy, high avidity might be needed for TCB to mediate the association between T cells and target cells. This association contributes to the T cell activation. So the different avidity may need to be considered when designing CD22 targeted CAR-T or TCB therapies. Besides, G5/44, BL22 and HA22 BsAbs with high internalization rate had better anti-tumor activity than HLL2, M971 and M972 BsAbs in this report, which indicated that the internalization of CD22-TCBs had less effect on their *in vitro* activity, as previously observed as well [24].

G5/44 BsAb with the best *in vitro* biological activity showed tumor inhibition *in vivo*, although the parent g5/44 mAb had no *in vivo* anti-tumor activity [27]. In this study, the moderate anti-tumor activity of G5/44 BsAb *in vivo* might be due to the low E:T ratio comparing to the other research [42] or G5/44 BsAb's high internalization rate. Besides, Fc-engineering by modulating affinity to FcRn at endosomal pH and extracellular pH could maintain the antibody/antigen complex at cell surface [60], which may contribute to the biological activity of TCB.

In conclusion, our study proved that TCB targeting CD22 could induce potent target cell lysis, T cell activation, T cell proliferation

and cytokine release *in vitro*, and anti-tumor activity *in vivo*. Additionally, we found that binding distal domain contributed to the avidity of IgG-[L]-scfv-like CD22-TCB to the target cells. Comparing with the antibody avidity to the target protein, the avidity to target cells further determined TCB's biological function. So, molecular structure, binding domain, as well as the avidity to protein and target cells should all be fully considered for the design of CD22-TCB to meet the requirement of patients with B-cell associated diseases.

Funding

Ethics approval

This study was carried out in strict accordance with the guidelines established by the Institutional Animal Care and Use Committee of the School of Shanghai Jiao Tong University.

Author contribution statement

Jianwei Zhu: Conceived and designed the experiments; Analyzed and interpreted the data; Contributed reagents, materials, analysis tools or data; Wrote the paper.

Jie Chen: Conceived and designed the experiments; Performed the experiments; Analyzed and interpreted the data; Contributed reagents, materials, analysis tools or data; Wrote the paper.

Zhidi Pan; Lei Han; Baohong Zhang; Mingyuan Wu; Yunsheng Yuan; Yanlin Bian: Analyzed and interpreted the data.

Junjun Liu; Yali Yue: Performed the experiments.

Xiaodong Xiao: Conceived and designed the experiments.

Hua Jiang; Yueqing Xie: Contributed reagents, materials, analysis tools or data.

Data availability statement

Data included in article/supp. material/referenced in article.

Declaration of competing interest

The authors declare that they have no known competing financial interests or personal relationships that could have appeared to influence the work reported in this paper

Acknowledgments

Appendix A. Supplementary data

Supplementary data to this article can be found online at https://doi.org/10.1016/j.heliyon.2023.e17960.

References

[1] M. Kalos, et al., T cells with chimeric antigen receptors have potent antitumor effects and can establish memory in patients with advanced leukemia, Sci. Transl. Med. 3 (95) (2011), 95ra73.

[2] J.N. Kochenderfer, et al., B-cell depletion and remissions of malignancy along with cytokine-associated toxicity in a clinical trial of anti-CD19 chimeric-antigen-receptor-transduced T cells, Blood 119 (12) (2012) 2709–2720.

[3] G. Salles, et al., Rituximab in B-cell hematologic malignancies: a review of 20 Years of clinical experience, Adv. Ther. 34 (10) (2017) 2232–2273.

[4] D.W. Lee, et al., Safety and response of incorporating CD19 chimeric antigen receptor T cell therapy in typical salvage regimens for children and young adults with acute lymphoblastic leukemia, Mol. Cancer Therapeut. 7 (5) (2015) 1164–1175.

[5] D.W. Lee, et al., T cells expressing CD19 chimeric antigen receptors for acute lymphoblastic leukaemia in children and young adults: a phase 1 dose-escalation trial, Lancet 385 (9967) (2015) 517–528.

[6] M. Xiong, et al., A novel CD3/BCMA bispecific T-cell redirecting antibody for the treatment of multiple myeloma, J. Immunother. 45 (2) (2022) 78–88.

[7] L.E. Budde, et al., Safety and efficacy of mosunetuzumab, a bispecific antibody, in patients with relapsed or refractory follicular lymphoma: a single-arm, multicentre, phase 2 study, Lancet Oncol. 23 (8) (2022) 1055–1065.

[8] T.F. Tedder, et al., CD22, a B lymphocyte-specific adhesion molecule that regulates antigen receptor signaling, Annu. Rev. Immunol. 15 (1997) 481–504.

[9] L. Nitschke, CD22 and Siglec-G: B-cell inhibitory receptors with distinct functions, Immunol. Rev. 230 (1) (2009) 128–143.

[10] R. Akazawa, et al., Inotuzumab ozogamicin is an effective treatment for CD22-positive acute undifferentiated leukemia: a case report, Pediatr. Blood Cancer 68 (5) (2021), e28976.

[11] N.N. Shah, et al., Characterization of CD22 expression in acute lymphoblastic leukemia, Pediatr. Blood Cancer 62 (6) (2015) 964–969.

[12] W. Haso, et al., Anti-CD22-chimeric antigen receptors targeting B-cell precursor acute lymphoblastic leukemia, Blood 121 (7) (2013) 1165–1174.

[13] J. Zhao, Y. Song, D. Liu, Clinical trials of dual-target CAR T cells, donor-derived CAR T cells, and universal CAR T cells for acute lymphoid leukemia, J. Hematol. Oncol. 12 (1) (2019) 17.

[14] S. Minguet, et al., Full activation of the T cell receptor requires both clustering and conformational changes at CD3, Immunity 26 (1) (2007) 43–54.

[15] P. Roda-Navarro, L. Alvarez-Vallina, Understanding the spatial topology of artificial immunological synapses assembled in T cell-redirecting strategies: a major issue in cancer immunotherapy, Front. Cell Dev. Biol. 7 (2019) 370.

[16] R. Sun, et al., A rational designed novel bispecific antibody for the treatment of GBM, Biomedicines 9 (6) (2021).

[17] S. Dickopf, G.J. Georges, U. Brinkmann, Format and geometries matter: structure-based design defines the functionality of bispecific antibodies, Comput. Struct. Biotechnol. J. 18 (2020) 1221–1227.

[18] B.H. Santich, et al., Interdomain spacing and spatial configuration drive the potency of IgG-[L]-scFv T cell bispecific antibodies, Sci. Transl. Med. 12 (534) (2020).

[19] M. Bacac, C. Klein, P. Umana, T.C.B. CEA, A novel head-to-tail 2:1 T cell bispecific antibody for treatment of CEA-positive solid tumors, OncoImmunology 5 (8) (2016), e1203498.

[20] J. Li, et al., Membrane-proximal epitope facilitates efficient T cell synapse formation by anti-FcRH5/CD3 and is a requirement for myeloma cell killing, Cancer Cell 31 (3) (2017) 383–395.

[21] G.J. Georges, et al., The Contorsbody, an antibody format for agonism: design, structure, and function, Comput. Struct. Biotechnol. J. 18 (2020) 1210–1220.

[22] C. Bluemel, et al., Epitope distance to the target cell membrane and antigen size determine the potency of T cell-mediated lysis by BiTE antibodies specific for a large melanoma surface antigen, Cancer Immunol. Immunother. 59 (8) (2010) 1197–1209.

[23] S.E. James, et al., Antigen sensitivity of CD22-specific chimeric TCR is modulated by target epitope distance from the cell membrane, J. Immunol. 180 (10) (2008) 7028–7038.

[24] S.S. Hoseini, et al., A potent tetravalent T-cell-engaging bispecific antibody against CD33 in acute myeloid leukemia, Blood Adv. 2 (11) (2018) 1250–1258.

[25] A. Lopez-Albaitero, et al., Overcoming resistance to HER2-targeted therapy with a novel HER2/CD3 bispecific antibody, OncoImmunology 6 (3) (2017), e1267891.

[26] Z. Wu, et al., Development of a tetravalent anti-GPA33/anti-CD3 bispecific antibody for colorectal cancers, Mol. Cancer Therapeut. 17 (10) (2018) 2164–2175.

[27] J.F. DiJoseph, et al., Antibody-targeted chemotherapy of B-cell lymphoma using calicheamicin conjugated to murine or humanized antibody against CD22, Cancer Immunol. Immunother. 54 (1) (2005) 11–24.

[28] J.P. Leonard, et al., Phase I/II trial of epratuzumab (humanized anti-CD22 antibody) in indolent non-Hodgkin's lymphoma, J. Clin. Oncol. 21 (16) (2003) 3051–3059.

[29] J.P. Leonard, et al., Epratuzumab, a humanized anti-CD22 antibody, in aggressive non-Hodgkin's lymphoma: phase I/II clinical trial results, Clin. Cancer Res. 10 (16) (2004) 5327–5334.

[30] F. Mussai, et al., Cytotoxicity of the anti-CD22 immunotoxin HA22 (CAT-8015) against paediatric acute lymphoblastic leukaemia, Br. J. Haematol. 150 (3) (2010) 352–358.

[31] G. Salvatore, et al., Improved cytotoxic activity toward cell lines and fresh leukemia cells of a mutant anti-CD22 immunotoxin obtained by antibody phage display, Clin. Cancer Res. 8 (4) (2002) 995–1002.

[32] X. Xiao, et al., Identification and characterization of fully human anti-CD22 monoclonal antibodies, mAbs 1 (3) (2009) 297–303.

[33] M. Lo, et al., Effector-attenuating substitutions that maintain antibody stability and reduce toxicity in mice, J. Biol. Chem. 292 (9) (2017) 3900–3908.

[34] J.R. Adair, et al., Humanization of the murine anti-human CD3 monoclonal antibody OKT3, Hum. Antibodies Hybridomas 5 (1–2) (1994) 41–47.

[35] J. Zhu, Mammalian cell protein expression for biopharmaceutical production, Biotechnol. Adv. 30 (5) (2012) 1158–1170.

[36] J. Zhu, Update on Production of Recombinant Therapeutic Protein: Transient Gene Expression, Smithers Rapra, 2013.

[37] K. Ding, et al., Production process reproducibility and product quality consistency of transient gene expression in HEK293 cells with anti-PD1 antibody as the model protein, Appl. Microbiol. Biotechnol. 101 (5) (2017) 1889–1898.

[38] M.S. Jiang, et al., Mammalian cell transient expression, non-affinity purification, and characterization of human recombinant IGFBP7, an IGF-1 targeting therapeutic protein, Int. Immunopharm. 29 (2) (2015) 476–487.

[39] H. Jiang, et al., Purification of clinical-grade disulfide stabilized antibody fragment variable–Pseudomonas exotoxin conjugate (dsFv-PE38) expressed in Escherichia coli, Appl. Microbiol. Biotechnol. 97 (2) (2013) 621–632.

[40] J. Chen, et al., A novel bispecific antibody targeting CD3 and Lewis Y with potent therapeutic efficacy against gastric cancer, Biomedicines 9 (8) (2021).

[41] L. Han, et al., Efficient generation of bispecific IgG antibodies by split intein mediated protein trans-splicing system, Sci. Rep. 7 (1) (2017) 8360.

[42] P.A. Moore, et al., Application of dual affinity retargeting molecules to achieve optimal redirected T-cell killing of B-cell lymphoma, Blood 117 (17) (2011) 4542–4551.

[43] S. Bang, et al., HA22 (R490A) is a recombinant immunotoxin with increased antitumor activity without an increase in animal toxicity, Clin. Cancer Res. 11 (4) (2005) 1545–1550.

[44] J. Carnahan, et al., Epratuzumab, a humanized monoclonal antibody targeting CD22: characterization of in vitro properties, Clin. Cancer Res. 9 (10 Pt 2) (2003) 3982S–3990S.

[45] J. Ereno-Orbea, et al., Molecular basis of human CD22 function and therapeutic targeting, Nat. Commun. 8 (1) (2017) 764.

[46] D. Fan, et al., Redirection of CD4+ and CD8+ T lymphocytes via an anti-CD3 x anti-CD19 bi-specific antibody combined with cytosine arabinoside and the efficient lysis of patient-derived B-ALL cells, J. Hematol. Oncol. 8 (2015) 108.

[47] K.C. Conlon, M.D. Miljkovic, T.A. Waldmann, Cytokines in the treatment of cancer, J. Interferon Cytokine Res. 39 (1) (2019) 6–21.

[48] Z. Pan, et al., Characterization of a novel bispecific antibody targeting tissue factor-positive tumors with T cell engagement, Acta Pharm. Sin. B 12 (4) (2022) 1928–1942.

[49] F. Lanza, et al., CD22 expression in B-cell acute lymphoblastic leukemia: biological significance and implications for inotuzumab therapy in adults, Cancers (Basel) 12 (2) (2020).

[50] L.L. Sun, et al., Anti-CD20/CD3 T cell-dependent bispecific antibody for the treatment of B cell malignancies, Sci. Transl. Med. 7 (287) (2015) 287ra70.

[51] Y. Zhou, et al., A novel bispecific antibody targeting CD3 and prolactin receptor (PRLR) against PRLR-expression breast cancer, J. Exp. Clin. Cancer Res. 39 (1) (2020) 87.

[52] J.F. de Vries, et al., The novel calicheamicin-conjugated CD22 antibody inotuzumab ozogamicin (CMC-544) effectively kills primary pediatric acute lymphoblastic leukemia cells, Leukemia 26 (2) (2012) 255–264.

[53] X. Du, et al., Differential cellular internalization of anti-CD19 and -CD22 immunotoxins results in different cytotoxic activity, Cancer Res. 68 (15) (2008) 6300–6305.

[54] R.F. Alderson, et al., CAT-8015: a second-generation pseudomonas exotoxin A-based immunotherapy targeting CD22-expressing hematologic malignancies, Clin. Cancer Res. 15 (3) (2009) 832–839.

[55] L. Sullivan-Chang, R.T. O'Donnell, J.M. Tuscano, Targeting CD22 in B-cell malignancies: current status and clinical outlook, BioDrugs 27 (4) (2013) 293–304.

[56] R.J. Kreitman, I. Pastan, Antibody fusion proteins: anti-CD22 recombinant immunotoxin moxetumomab pasudotox, Clin. Cancer Res. 17 (20) (2011) 6398–6405.

[57] A.R. Root, et al., Development of PF-06671008, a highly potent anti-P-cadherin/Anti-CD3 bispecific DART molecule with extended half-life for the treatment of cancer, Antibodies (Basel) 5 (1) (2016).

[58] Y. Wu, et al., Identification of human single-domain antibodies against SARS-CoV-2, Cell Host Microbe 27 (6) (2020) 891–898 e5.

[59] X. Tian, et al., Potent binding of 2019 novel coronavirus spike protein by a SARS coronavirus-specific human monoclonal antibody, Emerg. Microb. Infect. 9 (1) (2020) 382–385.

[60] R. Liu, et al., Fc-engineering for modulated effector functions-improving antibodies for cancer treatment, Antibodies (Basel) 9 (4) (2020).